PAPR Analyses for Broadband OFDM Transmitter with Digital IF Architecture

Zhenyu Zhang[a, b], Fengchun Tian[a], Fanxin Zeng[a, b], Guixin Xuan [a, b]
a. College of Communication Engineering, Chongqing University, Chongqing, China;
b. Chongqing Key Lab. of Emergency Communication, Chongqing Communication Institute, Chongqing, China.
zhenyu.zhang@cqu.edu.cn, fengchuntian@cqu.edu.cn, fzengx@cqu.edu.cn

***Abstract*-As one of main indexes of orthogonal frequency division multiplexing (OFDM) system, peak-to-average power ratio (PAPR) of the time-domain signal has an important effect on system performance. A larger PAPR has to require a wider linear range of power amplifier (PA) in system transmitter, which will greatly decrease the efficiency of PA. In this paper, we introduce a broadband OFDM communication system which is designed and implemented on the basis of digital intermediate frequency (IF) architecture and 1x4 multiple-input multiple-output (MIMO) technology. The parameters and structure of the 1x4 MIMO-OFDM communication system are provided, and its frequency spectrum and time signal are respectively tested. In addition, the PAPR problem is mainly analyzed, and the corresponding experimental results and simulation analyses are also presented.**

***Keywords*-OFDM; PAPR; MIMO; digital IF**

I. Introduction

Orthogonal frequency division multiplexing (OFDM) is a kind of multi-carrier (MC) modulation technique with a high spectral efficiency and resistance to multi-path fading [1]. When OFDM is combined with multiple-input multiple-output (MIMO) technique, the obtained MIMO-OFDM technique can provide higher transmission rate and/or transmission reliability, which leads to its wide applications in wireless communication systems, such as WiFi, WiMax, LTE and LTE-A [2]. In addition to the above public communication networks, MIMO-OFDM technique was also used to point-to-point transmission link, e. g., high frequency (HF) radio [3-4], video transmission [5], emergency service [6] and so on.

For MIMO-OFDM systems, many key technology points had been researched, such as symbol synchronization [7-8], carrier frequency offset estimation [9-11], multi-user detection [12-13], channel estimation [14-15], peak-to-average power ratio (PAPR) reduction [16-17], etc. These researches can provide helpful references for realization of specific MIMO-OFDM systems.

In this paper, we focus on the design and implementation of MIMO-OFDM systems. A set of 1x4 MIMO-OFDM transceiver with digital intermediate frequency (IF) architecture is introduced. The transceiver is designed for video transmission in emergency communication when communication infrastructure had been damaged in natural disaster. The designed MIMO-OFDM system consists of a vehicle platform with four antennas and multiple portable terminals with one antenna for each terminal. The command control center equipped with the vehicle platform can receive real-time video from different portable terminals which can be taken into disaster scene. Then, such system can be considered as an alternative to satellite emergency communication. Although satellite transmission has significant importance on emergency communication [18], the designed and implemented 1x4 MIMO-OFDM video transmission system can possess lower cost and larger flexibility.

For the presented 1x4 MIMO-OFDM communication system, we provide its design parameters and system structure. In addition, its frequency spectrum and time signal are respectively tested and analyzed. Also, we discussed the PAPR problem on the basis of baseband signal amplitude and IF signal envelope, and the corresponding experimental results and simulation analyses are also presented.

This paper can be organized as follows. We first introduce the designed and implemented broadband 1x4 MIMO-OFDM communication transceiver, where we present the detailed design scheme, system parameters and key technologies. Then the PAPR resistance is mainly analyzed in Section III. Finally, Section IV summarizes the results.

II. The Designed and Implemented Broadband MIMO-OFDM Communication System

A. Uplink Structure of the 1x4 MIMO-OFDM System

In order to provide video transmission for emergency communication, we design and implement a set of 1x4 MIMO-OFDM system whose uplink block diagram can be shown in Fig. 1.

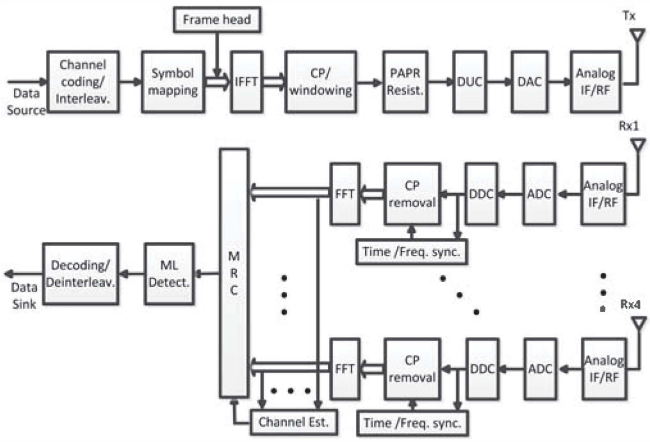

Fig. 1 Uplink block diagram of the designed and implemented 1x4 MIMO-OFDM video transmission system

978-1-4673-6544-4 /15/$31.00 ©2015 IEEE

The designed 1x4 MIMO-OFDM system employs digital IF structure with 30MHz transmitter IF frequency and 70MHz receiver IF frequency. For the digital processing part, there exist some basic components, such as convolutional coding/decoding, interleaving/deinterleaving, symbol mapping /maximum likelihood (ML) detection, inverse fast Fourier transform (IFFT)/FFT, frame head, cyclic prefix (CP), cyclic postfix, raised cosine window (RCW), PAPR resistance, channel estimation, time/frequency synchronization, maximum ratio combination (MRC), digital up conversion (DUC)/digital down conversion (DDC), digital to analog converter (DAC)/analog to digital converter (ADC), and so on.

In addition, the analog circuit part, namely analog IF and radio frequency (RF), mainly contains some typical components, such as automatic gain control (AGC) circuit, mixer, local oscillator (LO), power amplifier (PA), low-noise amplifier (LNA), bandpass filter (BPF), and so on. Fig.2 and 3 respectively show transmitter and receiver block diagrams, where Fig. 3 only gives one-channel case of the whole 4-channel receiver structure.

B. System Parameters

The main parameters of the designed and implemented 1x4 MIMO-OFDM video transmission system can be presented in Table I. The whole 8MHz system bandwidth (from 336MHz to 344MHz) is divided into 4 channels with each channel possessing 2MHz bandwidth, and different channel can be assigned to different portable terminal. The corresponding central frequencies of 4 channels are 337, 339, 341 and 343MHz, respectively. Each channel can be further divided into 64 subcarriers and then the subcarrier frequency spacing Δf is equal to 31.25kHz, namely $64\times 31.25Hz = 2MHz$. In fact, there exist one null subcarrier for direct current and 11 subcarriers for guard band, and there are only 48 data subcarriers and 4 polit subcarriers.

We choose 128-point IFFT/FFT and IFFT/FFT period is equal to 32μs, namely 1/(31.25kHz)= 32μs. A long CP duration of 8μs is designed to resist to multi-path interference (MPI), which is equal to a quarter of IFFT/FFT period. The corresponding number of CP points is 32, namely 128/4=32. Hence the symbol duration of 1x4 MIMO-OFDM system is 32μs+8μs =40μs and the number of symbol samples in time domain is 128+32=160. For the windowing operation, a cyclic postfix with 1.25μs and 5 sample points is used. The roll off factor of RCW is 0.03125. By combining 5-point cyclic postfix with 160-point OFDM symbol, the whole length of the RCW is 165, and the corresponding windowing coefficients S_{win} can be expressed as

$$S_{win} = \big(0,0.0955,0.3455,0.6545,0.9045,\overbrace{1,1,\cdots,1}^{155},0.9045,0.6545,0.3455,0.0955,0\big) \quad . \quad (1)$$

For the implemented 1x4 MIMO-OFDM communication system, there exist three convolutional coding rates in total, namely 1/2, 2/3 and 3/4. Combining three channel coding rates with quadrature phase-shift keying (QPSK) modulation, we can obtain different data transmission rates, which is helpful for the tradeoff between transmission rate and transmission reliability.

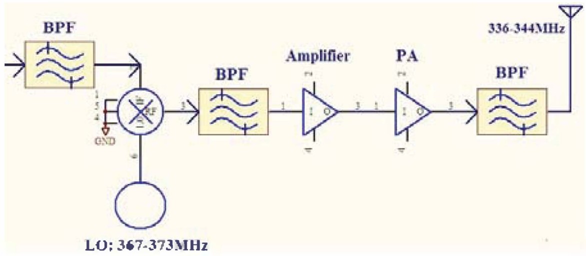

Fig. 2 Block diagram of analog circuit part of 1x4 MIMO-OFDM transmitter

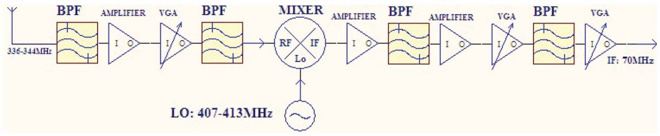

Fig. 3 Block diagram of analog circuit part of the 1x4 MIMO-OFDM receiver (single antenna)

TABLE I
PARAMETERS OF THE DESIGNED 1X4 MIMO-OFDM SYSTEM

Parameter	Value
Frequency range of RF	336-344MHz
Channel bandwidth	2MHz
Four central frequencies of RF	337, 339, 341, 343MHz
Number of data subcarriers	48
Number of subcarriers in total	52
IFFT/FFT size	128
IFFT/FFT period	32μs
Subcarrier frequency spacing	31.25kHz
CP duration	8μs
Cyclic postfix duration	1.25μs
Symbol duration	40μs
Roll off factor of RCW	0.03125
Symbol mapping	QPSK
Convolutional coding rate	1/2, 2/3, 3/4
Transmitter/receiver IF frequency	30MHz/70MHz
DAC/ADC sampling rate	160MSPS/40MSPS
Mean power of portable terminal	5W

C. Development platform

The baseband/IF design of 1x4 MIMO-OFDM communication system is based on field programmable gate array (FPGA) devices and the corresponding XILINX ISE software. We use two Virtex-5 XC5VSX50T FPGAs for vehicle platform and one Virtex-4 XC4VLX25 FPGA for portable terminal. For vehicle platform, four high performance ADCs (AD9246 with 14-bit and 80MSPS) and one high performance DAC (AD9744 with 16-bit and 210MSPS) are used. For portable terminal, we utilize one ADC (AD6640 with 12-bit and 65MSPS) and the same DAC as vehicle platform.

D. IF and RF Spectrum Analyses

For the implemented 1x4 MIMO-OFDM video transmission system, the central frequency shifting of signal is completed by using DUC/DDC for IF and mixer/LO for RF. We use two main components, namely cascaded integrator-comb (CIC) filter and direct digital synthesizer (DDS), to realize DUC and DDC. DUC implements the conversion of complex digital baseband signal to a real digital IF signal and DDC operates the inverse processing.

At transmitter, the digital IF frequency is equal to 30MHz and DAC sampling rate is 160MSPS. Then we can depict the power spectrum density (PSD) curve in Fig. 4. In order to further show RF spectrum, we test the case of 339MHz central frequency, which is presented in Fig.5. At receiver, the 10MHz digital IF signal can be generated after ADC since analog IF frequency is 70MHz and ADC sampling rate is 40MHz, which is shown in Fig. 6.

III. Analyses of PAPR Performance

As one of main drawbacks of OFDM modulation, high PAPR will reduce the efficiency of PA. For an OFDM system, the *i*-th OFDM time-domain symbol with *N*-point IFFT can be calculated by

$$x_{i,n} = \frac{1}{\sqrt{N}} \sum_{k=0}^{N-1} X_{i,k} e^{j\frac{2\pi nk}{N}}, 0 \le n \le N-1, \qquad (2)$$

where $\{X_{i,k}, 0 \le k \le N-1\}$ denotes a set of zero-padding complex data symbols transmitted in the *i*-th OFDM symbol. Then, the definition of PAPR of the *i*-th OFDM symbol can be expressed as

$$PAPR_i = 10\lg \frac{\max\limits_{0\le n\le N-1} |x_{i,n}|^2}{E\left[|x_{i,n}|^2\right]} \ (\text{dB}), \qquad (3)$$

where $E[\cdot]$ is the statistical expectation operator. The notations of $\max\limits_{0\le n\le N-1} |x_{i,n}|^2$ and $E\left[|x_{i,n}|^2\right]$ represent peak power and average power of the *i*-th OFDM symbol, respectively.

According to (3), the PAPR is defined on the basis of the absolution value of baseband signal. However, it is well known that PA only amplifies RF analog signal, not baseband digital signal. In fact, for baseband time-domain signal $x_{i,n}$, the corresponding RF analog signal $x_{RF}(t)$ with central frequency f_0 can be expressed as

$$x_{RF}(t) = \text{Re}[x_{i,n}] \cdot \cos(2\pi f_0 t) - \text{Im}[x_{i,n}] \cdot \sin(2\pi f_0 t), \qquad (4)$$

where $\text{Re}[x_{i,n}]$ and $\text{Im}[x_{i,n}]$ denote the real part and imaginary part of $x_{i,n}$, respectively.

The equation (4) can be further calculated as

$$x_{RF}(t) = V(t) \cdot \cos(2\pi f_0 t + \theta(t)), \qquad (5)$$

where $V(t)$ and $\theta(t)$ represent envelope and phase of $x_{RF}(t)$, respectively, and can be given by

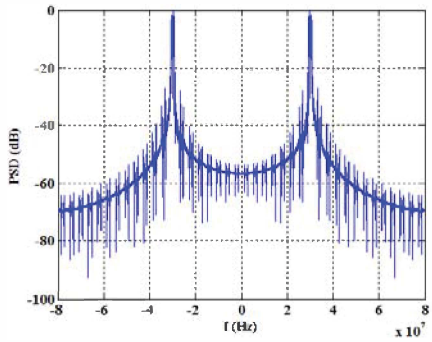

Fig. 4 The 30MHz-IF PSD of the designed 1x4 MIMO-OFDM transmitter

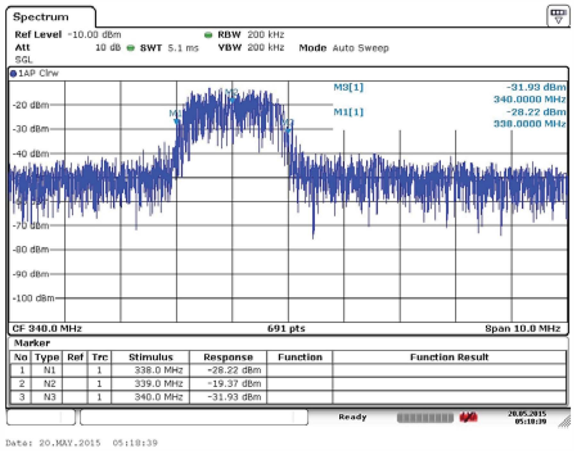

Fig. 5 The 339MHz-RF PSD of the designed 1x4 MIMO-OFDM transmitter

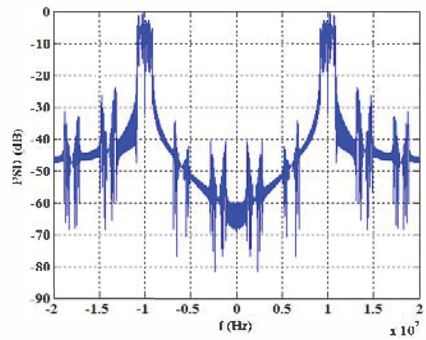

Fig. 6 PSD of the designed 1x4 MIMO-OFDM receiver after ADC with 70MHz IF frequency and 40MSPS sampling rate

$$\begin{cases} V(t) = \sqrt{\text{Re}^2[x_{i,n}] + \text{Im}^2[x_{i,n}]} \\ \theta(t) = \arctan \dfrac{\text{Im}[x_{i,n}]}{\text{Re}[x_{i,n}]} \end{cases}. \qquad (6)$$

From (6), it is obvious that the envelope of RF analog signal $x_{RF}(t)$ is the same as the absolution value of baseband signal $x_{i,n}$. As a result, we can resist PAPR at the baseband although PA amplifies the envelope of RF analog signal. For the designed 1x4 MIMO-OFDM system, we depict the absolution value curve of any OFDM symbol with 40μs duration in Fig. 7

and the corresponding IF signal curve with IF frequency 30MHz in Fig. 8, respectively. Comparing two figures, we can see that the envelope curve is accordant with absolution value curve. In order to resist PAPR, we design specific frame head symbols with 4dB maximum PAPR and clip the data peak value down to 8dB PAPR, which can be shown in Fig. 9.

IV. Conclusions and Future Work

The paper presents the results of the design and implement of a 1x4 MIMO-OFDM video transmission system. We provide unlink structure, system parameters, development platform and IF/RF spectrum analyses. Also, the corresponding PAPR problem is mainly discussed. The following work will focus on video transmission reliability, and the direct sequence spread spectrum technique will be experimented on the same development platform.

Acknowledgment

This work was supported by National Natural Science Foundation of China (NSFC) under Grants 61471366, 61002034, 61271003, and 61271251, China Postdoctoral Science Foundation Grants 2015T80959 and 2014M552318, Natural Science Foundation Project of CQ Grant cstc2014jcyjA40050, and Chongqing Postdoctoral Science Special Foundation Grant Xm2014031.

References

[1] F. Gregorio, J. Cousseau, S. Werner, T. Riihonen, and R.Wichman, "EVM analysis for broadband OFDM direct-conversion transmitters," *IEEE Trans. Veh. Technol.*, vol. 62, no. 7, pp. 3443-3451, July 2013.

[2] Y. S. Cho, J. Kim, W. Y. Yang, et al. MIMO-OFDM wireless communications with MATLAB. John Wiley & Sons, 2010.

[3] P. M. Ndao, Y. Erhel, D. Lemur, and J. Le Masson, "Design of a high-frequency (3-30MHz) multiple-input multiple-output system resorting to polarisation diversity," IET Microwaves, Antennas & Propagation, vol. 5, no. 11, pp. 1310-1318, Aug. 2011.

[4] B.A. Witvliet, E. van Maanen, G.J. Petersen, etal. "The importance of circular polarization for diversity reception and MIMO in NVIS propagation," Proc. of the 8th European Conference on Antennas and Propagation, pp. 2797-2801, 2014.

[5] N. F. Fan, Y. Liu and L. Zhang, "Hybrid digital-analog video transmission based on H.264/AVC and ParCast in MIMO-OFDM WLANs," Proc. of the 21st International Conference on Telecommunications, pp. 395-399, 2014.

[6] Z. G. Yang, "Research on the key techniques of wireless communication for emergency information system,"Proc. of the 3rd International Conference on Computer Science and Information Technology, vol.7, pp. 432-435, 2010.

[7] D. W. Bliss and P. A. Parker, "Temporal Synchronization of MIMO Wireless Communication in the Presence of Interference," IEEE Transactions on Signal Processing, vol. 58, no. 3, pp.1794-1806, 2010.

[8] T. Y. Hsu and S. Y. Cheng, "Low-Complexity Sequential Searcher for Robust Symbol Synchronization in OFDM Systems," IEEE Transactions on Very Large Scale Integration Systems, vol. 20, no. 5, pp.959-963, 2012.

[9] A. Bannour, Y. C. Sun, M. L. Ammari, etal, "A Novel Algebraic Carrier Frequency Offset Estimator for ASTC-MIMO-OFDM Systems Over a Correlated Frequency-Selective Channel," IEEE Transactions on Vehicular Technology, vol. 61, no. 6, pp.2468-2475, 2012.

[10] Y. J. Liang, G. L. Stuber, J. F. Chang and D. N. Yang, "Joint Channel and Frequency Offset Estimator for the Downlink of Coordinated MIMO-OFDM Systems," IEEE Transactions on Wireless Communications, vol. 11, no. 6, pp.2254-2265, 2012.

[11] A. K. Dutta, K. V. S. Hari and L. Hanzo, "Minimum-Error-Probability CFO Estimation for Multiuser MIMO-OFDM Systems," IEEE Transactions on Vehicular Technology, vol. 64, no. 7, pp.2804-2818, 2015.

[12] C. Studer and E. G. Larsson, "PAR-Aware Large-Scale Multi-User MIMO-OFDM Downlink," IEEE Journal on Selected Areas in Communications, vol. 31, no. 2, pp.303-313, 2013.

[13] S. Wu, L. L. Kuang, Z. Y. Ni, etal, " Low-Complexity Iterative Detection for Large-Scale Multiuser MIMO-OFDM Systems Using Approximate Message Passing," IEEE Journal of Selected Topics in Signal Processing, vol. 8, no. 5, pp.902-915, 2014.

[14] Z. Gao, L. L. Dai, Z. H. Lu, etal, "Super-Resolution Sparse MIMO-OFDM Channel Estimation Based on Spatial and Temporal Correlations," IEEE Communications Letters, vol. 18, no. 7, pp.1266-1269, 2014.

[15] W. B. Ding, F. Yang, W. Dai and J. Song, "Time–Frequency Joint Sparse Channel Estimation for MIMO-OFDM Systems," IEEE Communications Letters, vol. 19, no. 1, pp.58-61, 2015.

[16] Y. C. Hung and S. H. Tsai, "PAPR Analysis and Mitigation Algorithms for Beamforming MIMO OFDM Systems," IEEE Transactions on Wireless Communications, vol. 13, no. 5, pp.2588-2600, 2014.

[17] S. J. Ku, "Low-Complexity PTS-Based Schemes for PAPR Reduction in SFBC MIMO-OFDM Systems," IEEE Transactions on Broadcasting, vol. 60, no. 4, pp.650-658, 2014.

[18] T. Pecorella, L. S. Ronga, F. Chiti, etal, "Emergency satellite communications: research and standardization activities," IEEE Communications Magazine, vol. 53, no. 5, pp. 170-177, 2015.

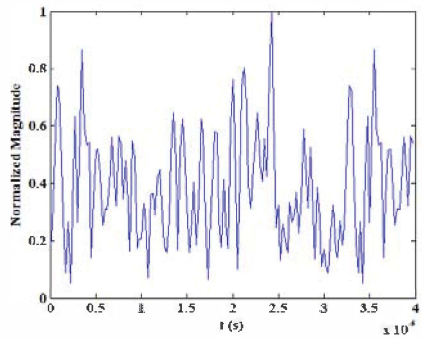

Fig. 7 The absolute value curve of any OFDM symbol with 40μs duration for the implemented 1x4 MIMO-OFDM system

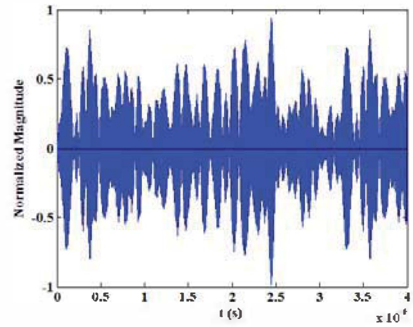

Fig. 8 The corresponding IF signal curve with IF frequency 30MHz for the implemented 1x4 MIMO-OFDM system

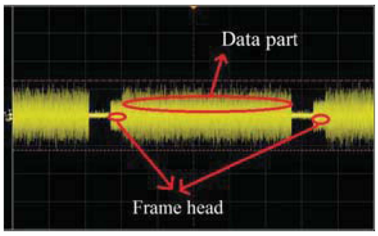

Fig. 9 RF signal curve (consisting of frame head and data part) for the implemented 1x4 MIMO-OFDM system